Oxidation of *p*-chlorotoluene and cyclohexene catalysed by polymer-anchored oxovanadium(IV) and copper(II) complexes of amino acid derived tridentate ligands†

Mannar R. Maurya,*[a] Maneesh Kumar,[a] Amit Kumar[b] and João Costa Pessoa*[b]

Received 20th March 2008, Accepted 2nd June 2008
First published as an Advance Article on the web 11th July 2008
DOI: 10.1039/b804823a

3-Formylsalicylic acid (Hfsal), covalently bound to chloromethylated polystyrene (PS) and cross-linked with 5% divinylbenzene reacts with D,L-alanine and L-isoleucine to give the Schiff-base tridentate ligands PS–H_2fsal–D,L-Ala and PS–H_2fsal–L-Ile, respectively. These anchored ligands upon reaction with $VOSO_4$ and $Cu(CH_3COO)_2\cdot H_2O$ form the complexes PS–[VO(fsal–D,L-Ala)(H_2O)], PS–[Cu(fsal–D,L-Ala)(H_2O)], PS–[VO(fsal–L-Ile)(H_2O)] and PS–[Cu(fsal–L-Ile)(H_2O)]. The structures of these immobilized complexes have been established on the basis of scanning electron micrographs, spectroscopic (infrared, electronic and EPR), thermogravimetric and elemental analysis studies. The oxidation of *p*-chlorotoluene and cyclohexene has been investigated using these complexes as the catalysts in the presence of H_2O_2 as the oxidant. Reaction conditions have been optimised by considering the concentration of the oxidant, the amount of catalyst used and the temperature of the reaction mixture. Under the optimised conditions, *p*-chlorotoluene gave a maximum of 14% conversion using PS–[VO(fsal–D,L-Ala)(H_2O)] as the catalyst, with the main products having a selectivity order of: *p*-chlorobenzaldehyde >> *p*-chlorobenzylalcohol > *p*-chlorobenzoic acid > 2-methyl-5-chlorophenol > 3-methyl-6-chlorophenol. The oxidation of cyclohexene with PS–[VO(fsal–D,L-Ala)(H_2O)] proceeds with 79% conversion, which is followed by PS–[VO(fsal–L-Ile)(H_2O)] with 77% conversion, and the oxidation of cyclohexene by Cu-based catalysts occurs with considerably lower conversions (29–32%). The selectivity of the products follows the order: 2-cyclohexene-1-ol > cyclohexene oxide > cyclohexane-1,2-diol > 2-cyclohexene-1-one. Recycling studies indicate that these catalysts can be reused at least three times without any significant loss in their catalytic potential. However, EPR studies indicate that while the polymer supported V(IV)O-complexes do not change after being used, the EPR spectra of the Cu-complexes show significant changes. The corresponding non-polymer bound complexes [VO(fsal–D,L-Ala)(H_2O)], [Cu(fsal–D,L-Ala)(H_2O)], [VO(fsal–L-Ile)(H_2O)] and [Cu(fsal–L-Ile)(H_2O)] have also been prepared in order to compare their spectral properties and catalytic activities. The non-polymer bound complexes exhibit lower conversion, along with lower turn-over frequency as compared to their polymer-bound analogues. Several EPR, ^{51}V NMR and UV-vis studies have been undertaken to detect the intermediate species, and outlines for the mechanisms of the catalytic reactions are proposed.

Introduction

Vanadium and copper are important elements in biology and in inorganic and organic synthesis, and can heterogeneously or homogeneously catalyse the selective oxidations of alkanes, alkenes, arenes, alcohols, halides, sulfides, *etc.*[1–3] Hydrogen peroxide is a clean and readily available oxidant and is, together with molecular oxygen, one of the preferred oxidants for laboratory or industrial reactions. The electron-rich peroxide group easily forms complexes with metal ions of low d^n configurations, such as vanadium and molybdenum, and a number of these complexes are good oxidants. Namely, vanadium peroxide complexes are effective oxidants in non-protic solvents under mild conditions and not only catalyse the epoxidation of olefins, but also hydroxylate aromatic hydrocarbons and alkanes to yield alcohols and ketones.[4]

Immobilisation of the complexes in solid supports often presents advantages for industrial applications, and the catalytic potentials of polymer-immobilised metal complexes in organic transformations have been reviewed in detail by several groups.[5–8] This type of immobilisation of active metal complexes has evolved as a promising strategy for combining the advantages of homogeneous as well as heterogeneous catalysts, due to their easy separation from the products by simple filtration, and to meet the industrial demand of recyclability for continuous operation.[9,10]

Amino acids immobilised on Merrifield resin were reported by Petit and Jozefonvicz, and later by Valodker *et al.*[11,12] Due

---

[a] *Department of Chemistry, Indian Institute of Technology Roorkee, Roorkee-247667, India. E-mail: rkmanfcy@iitr.ernet.in*
[b] *Centro Química Estrutural, Instituto Superior Técnico, TU Lisbon, Av Rovisco Pais, 1049–001 Lisboa, Portugal. E-mail: pcjpessoa@popsrv.ist.utl.pt*

† Electronic supplementary information (ESI) available: EDAX, IR spectral data, spin Hamiltonian parameters, ^{51}V NMR chemical shifts and electronic spectra. For ESI see DOI: 10.1039/b804823a

to the presence of the reactive amino, as well as carboxylic acid groups, special reagents were required to achieve immobilisation either through the amino group or the carboxylato group. We have simplified the procedure of immobilisation by reacting chloromethylated polystyrene with 3-formylsalicylic acid in the first step followed by condensation of an amino acid with immobilised 3-formylsalicylic acid.[13] In this way the ligand obtained has more coordination sites available to bind to the metal ion, which in turn may improve the catalytic activity and turn-over rates for the catalysts. As a continuation of our work on the development of such heterogeneous catalysts we recently reported PS–[VO(fsal–β-Ala)(DMF)] (where H_2fsal–β-Ala = Schiff base derived from 3-formylsalicylic acid and β-alanine, PS = polystyrene, DMF = dimethylformamide) immobilised on polystyrene and explored for their catalytic potential in the oxidation of a series of organic substrates. We report here the immobilisation of oxovanadium(IV) and copper(II) complexes of the dibasic tridentate oxygen and nitrogen donor ligands, H_2fsal–D,L-Ala and H_2fsal–L-Ile (Scheme 1), along with their catalytic activities for the oxidation of *p*-chlorotoluene and cyclohexene.

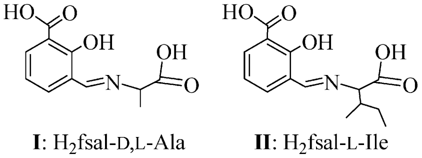

I: H_2fsal-D,L-Ala **II**: H_2fsal-L-Ile

Scheme 1

Selective oxidation of *p*-chlorotoluene (PCT) to *p*-chlorobenzaldehyde (CBD) is an important reaction as CBD is a key intermediate in the synthesis of a variety of fine chemicals, such as pharmaceutical drugs, dyes, optical brighteners and agricultural chemicals.[14] Traditionally, *p*-chlorobenzaldehyde is produced mainly from the chlorination of *p*-chlorotoluene, which forms *p*-chlorobenzalchloride and is then subjected to acid hydrolysis.[15] It can also be produced by the hydrogenation of *p*-chlorobenzonitrile.[16] Industrial methods use the oxidation of *p*-chlorotoluene catalysed by soluble transition metal acetates to give a mixture of *p*-chlorobenzyl alcohol and *p*-chlorobenzaldehyde, with further oxidation of *p*-chlorobenzyl alcohol also yielding *p*-chlorobenzaldehyde.[17–20] Vanadium silicate molecular sieves also catalyse a variety of reactions but only a limited number of literature citations have been reported for the liquid-phase oxidation of *p*-chlorotoluene using the clean and green oxidant H_2O_2.[21,22]

The catalytic epoxidation of unsaturated hydrocarbons represents an industrially important synthetic method for the production of speciality and fine chemicals. Polymer-supported transition metal complexes with Schiff-bases have been shown to be active catalysts for the epoxidation of olefinic compounds in the presence of hydrogen peroxide/*tert*-butyl hydroperoxide as oxidants.[23–26]

Vanadium(IV) is a d^1 metal ion and copper(II) has a d^9 configuration, and in many spectroscopic studies they have been compared using the hole-formalism.[27] Both have one unpaired electron and electron paramagnetic resonance is a particularly good and relatively simple spectroscopic method to study their complexes. In this work, we therefore explore both the adequate capacity of V and Cu complexes to catalyse oxidation reactions and the rich information that may be obtained from their EPR spectra.

Experimental

Materials and methods

V_2O_5 (S.D. Fine Chemicals, India), cupric acetate monohydrate, $VOSO_4\cdot5H_2O$, salicylic acid, hexamine (Loba Chemie, India), benzene, barium chloride, sodium hydroxide (Ranbaxy, India), D,L-alanine and L-isoleucine (Spectrochem, India) were used as obtained. Chloromethylated polystyrene [18.9% Cl, 5.3 mmol Cl per gram of resin] having 5% cross-linking with divinylbenzene was obtained as a gift from Thermax Limited, Pune, India. 3-Formylsalicylic acid was prepared according to a method reported in the literature.[28]

Elemental analyses of the compounds were carried out using an Elementar model Vario-El-III. An inductively-coupled plasma spectrometer (ICP, Labtam 8440 plasmalab) was used for the analysis of copper and vanadium after leaching the metal ions with conc. nitric acid and diluting with distilled water (for copper), or with a very dilute aqueous KOH solution (for vanadium) to a specific volume in volumetric flasks. Thermogravimetric analyses of the complexes were carried out using a Perkin-Elmer (Pyris Diamond) instrument in air with a rate of 10 °C min^{-1}. Field emission scanning electron microscopy (FE-SEM) and energy dispersive X-ray analysis (EDAX) plots of anchored complexes were recorded using a FEI Quanta 200 FEG microscope, The Netherlands. Chloromethylated polystyrene with a known chlorine content (see above) was used as a reference. The samples were dusted on alumina and coated with a thin film of gold to make the surface conductive, to prevent surface charging and to protect the surface material from thermal damage by the electron beam. IR spectra were recorded as KBr pellets on a Nicolet NEXUS Aligent 1100 series FT-IR spectrometer. Electronic spectra of both the ligands and complexes were recorded in nujol on a Shimadzu 1601 UV-visible spectrophotometer by layering the mull of the sample on the inside of one of the cuvettes. The inside of the other cuvette was layered with Nujol and used as the reference. The EPR spectra were recorded using a Bruker ESP 300E X-band spectrometer. For the samples containing the polymer-anchored complex, the spectra were measured at room temperature and also at 77 K after swelling in DMF; for the non-polymer-bound complexes, the samples in either DMF or MeOH were frozen in liquid nitrogen, and the EPR spectra were measured at 77 K. The spin Hamiltonian parameters were obtained by simulation of the spectra with the computer program by Rockenbauer and Korecz.[29] The ^{51}V NMR spectra were recorded on a Bruker Avance III 400 Mhz instrument. A Thermax Nicolet gas chromatograph with a HP-1 capillary column (30 m × 0.25 μm × 0.25 μm) was used to analyse the reaction products and their quantifications were made on the basis of the relative peak area of the respective product. Each catalytic experiment was repeated twice for the validity of data. The identity of the products was confirmed using GC-MS, model Perkin-Elmer Clarus 500 by comparing the fragments of each product with the library that was available.

Preparations

Preparation of PS–Hfsal. Chloromethylated polystyrene (10 g) was allowed to swell in DMF (50 mL) for 2 h. A solution of 3-formylsalicylic acid (16.6 g, 0.10 mol) in DMF (40 mL) was added to the above suspension followed by triethylamine (15 g) in ethylacetate (50 mL), and the reaction mixture was then heated to 90 °C for 10 h whilst stirring continuously. After cooling to room temperature, the yellowish resin was separated by filtration, washed with hot DMF (3 × 5 mL) and followed by hot ethanol. The whole process was repeated with 5 g of 3-formyl salicylic acid and the PS–Hfsal thus obtained was dried in an air oven at *ca.* 120 °C.

Preparation of PS–H_2fsal–D,L-Ala III. The polymer-bound, PS–Hfsal (5.0 g) was allowed to swell for 3 h in water (100 mL). A solution of D,L-alanine (4.71 g, 0.053 mol) and KOH (2.96 g, 0.053 mol) in water (20 mL) was added to the above suspension and the reaction mixture was allowed to stir in an oil bath at *ca.* 90 °C for 12 h. After cooling to room temperature, the solid resin beads were filtered, washed thoroughly with water followed by ethanol and dried under vacuum. (Found: C 75.28, H 8.08, N 3.01%).

Preparation of PS–H_2fsal–L-Ile IV. The PS–H_2fsal–L-Ile was synthesised similarly using PS–Hfsal (5.0 g) with L-isoleucine (6.94 g, 0.053 mol). (Found: C 71.72, H 9.61, N 3.29%).

Preparation of PS–[VO(fsal–D,L-Ala)(H_2O)] 1. The polymer-anchored ligand PS–H_2fsal–D,L-Ala (2.5 g) was allowed to swell in methanol (30 mL) for 2 h. Vanadyl sulfate (6.70 g, 0.0265 mol) dissolved in 30 mL of methanol/water (7:3) was added to the above suspension and the reaction mixture was refluxed in an oil bath with continuous mechanical stirring for 70 h. The greenish resin beads were separated by filtration, washed thoroughly with hot methanol and dried in an air oven at *ca.* 120 °C. (Found: C 65.55, H 7.58, N 1.82, V 5.43%).

Preparation of PS–[Cu(fsal–D,L-Ala)(H_2O)] 2. A methanolic solution of $Cu(CH_3COO)_2 \cdot H_2O$ (5.0 g, 0.025 mol in 20 mL) was added to a suspension of PS–H_2fsal–D,L-Ala (2.5 g) in methanol (30 mL) as described above, and the reaction mixture was refluxed in an oil bath for 72 h. After cooling to ambient temperature, the coloured resin beads were filtered, washed with hot methanol and dried in an air oven at *ca.* 120 °C. (Found: C 68.64, H 7.09, N 1.76, Cu 6.47%).

Preparation of PS–[VO(fsal–L-Ile)(H_2O)] 3 and PS–[Cu(fsal–L-Ile)(H_2O)] 4. Complexes **3** and **4** were prepared similarly as described for **1** and **2**, respectively. Compound **3**: (found: C 66.38, H 7.85, N 1.56, V 4.56%). Compound **4**: (found: C 67.77, H 9.03, N 1.86, Cu 6.16%).

Preparation of [VO(fsal–D,L-Ala)(H_2O)] 5. A solution of 3-formylsalicylic acid (1.66 g, 0.010 mol) dissolved in 10 mL of water was added to a solution of D,L-alanine (0.89 g, 0.010 mol) and KOH (0.56 g, 0.010 mol in 20 mL). The reaction mixture was stirred for 2 h and a yellow solution was obtained. An aqueous solution of vanadyl sulfate (2.53 g, 0.010 mmol in 30 mL) was added slowly and digested on a water bath for 3 h. After reducing the volume to *ca.* 10 mL and keeping at *ca.* 10 °C overnight, a green solid separated out which was filtered, washed with diethyl ether and dried in a vacuum desiccator. Yield 55%. (Found: C 41.02, H 3.54, N 4.26, V 15.62. Calcd for $C_{11}H_{11}O_7NV$: C 41.25, H 3.44, N 4.38, V 15.94%).

Preparation of [Cu(fsal–D,L-Ala)(H_2O)] 6. The ligand H_2fsal–D,L-Ala (0.010 mol) was prepared *in situ* as described in the preparation for **5**, except an aqueous solution of $Cu(CH_3COO)_2 \cdot H_2O$ (2.0 g, 0.010 mol in 20 mL) was added. The reaction mixture was digested on a water bath for 3 h. After being kept at ambient temperature, the green solid that had slowly separated out was filtered, washed with water followed by diethyl ether and dried in a vacuum desiccator. Yield: 62%. (Found: C 41.33, H 3.37, N 4.36, Cu 19.84. Calcd for $C_{11}H_{11}O_6NCu$: C 41.70, H 3.48, N 4.42, Cu 20.07%).

Preparation of [VO(fsal–L-Ile)(H_2O)] 7 and [Cu(fsal–L-Ile)(H_2O)] 8. The ligand H_2fsal–L-Ile was prepared *in situ* as stated above. Complexes of **7** and **8** were prepared in about 60% yield, which was similar to **5** and **6**, respectively, replacing H_2fsal–D,L-Ala with H_2fsal–L-Ile. Complex **7**: (found: C 46.61, H 4.82, N 3.66, V 13.81. Calcd for $C_{14}H_{17}O_7NV$: C 46.42, H 4.73, N 3.87, V 14.06%). Complex **8**: (found: C 46.93, H 4.87, N 3.82, Cu 17.46. Calcd for $C_{14}H_{17}O_6NCu$: C 46.86, H 4.78, N 3.90, Cu 17.71%).

Elemental analysis data for the ligands and complexes are presented in the experimental section. The metal and ligand loading in polymer-anchored complexes is presented in Table 1.

Catalytic activity studies

All catalysts were allowed to swell in acetonitrile for 2 h prior to their use for the catalytic reactions.

Oxidation of *p*-chlorotoluene. In a typical reaction, an aqueous 30% H_2O_2 solution (2.27 g, 0.020 mol), *p*-chlorotoluene (1.126 g, 010 mol) and the catalyst (0.025 g) were mixed in CH_3CN (15 mL), and the reaction mixture was heated at 80 °C with continuous stirring in an oil bath. The progress of the reaction was monitored as a function of time by withdrawing portions of the sample and analyzing it quantitatively by gas chromatography. The identities of the products were confirmed by GC-MS.

Table 1 Analytical data for polymer-loading of both the ligand and complexes

Compounds	Ligand loading/mmol g^{-1} resin	Metal ion loading/mmol g^{-1} resin	Ligand : metal ratio
PS–H_2fsal–D,L-Ala	2.15	—	—
PS–[VO(fsal–D,L-Ala)(H_2O)]	1.32	1.06	1.2 : 1
PS–[Cu(fsal–D,L-Ala)(H_2O)]	1.26	1.01	1.2 : 1
PS–H_2 fsal–L-Ile	2.35	—	—
PS–[VO(fsal–L-Ile)(H_2O)]	1.11	0.89	1.2 : 1
PS–[Cu(fsal–L-Ile)(H_2O)]	1.33	0.97	1.3 : 1

Oxidation of cyclohexene. The catalytic oxidation of cyclohexene was also carried out using all catalysts. Cyclohexene (0.82 g, 0.010 mol), aqueous 30% H_2O_2 (2.27 g 0.020 mol) and the catalyst (0.025 g) were mixed in acetonitrile (20 mL), and the reaction mixture was heated at 80 °C with continuous stirring. The reaction products were analysed and identified as mentioned above.

Results and discussion

The synthesis of the polymer-anchored ligands involved two steps. In the first step, chloromethylated polystyrene, cross-linked with 5% divinylbenzene reacted with 3-formylsalicylic acid in the presence of triethylamine in ethylacetate to give the polymer-anchored 3-formylsalicylic acid, PS–Hfsal. During the reaction, the COOH group of 3-formylsalicylic acid reacts with the CH_2Cl group of the chloromethylated polystyrene. The second step involves the reaction between PS–Hfsal and D,L-alanine or L-isoleucine in the presence of potassium hydroxide to give the polymer-anchored ligands, PS–H_2fsal–D,L-Ala (**III**) and PS–H_2fsal–L-Ile (**IV**). The whole synthetic procedure considering PS–H_2fsal–D,L-Ala (**III**) as a representative example is presented in Scheme 2. The loading of the ligands was confirmed from estimating the amount of chlorine that remained present after forming the anchored ligands. Thus, the remaining chlorine content of 0.5 and 0.4% determined gravimetrically in PS–H_2fsal–D,L-Ala and PS–H_2fsal–L-Ile, respectively suggests a nearly quantitative loading of ligands.

The polymer-anchored ligands **III** and **IV** reacted with $VOSO_4$ in methanol–water and formed the polymer-bound oxovanadium(IV) complexes PS–[VO(fsal–D,L-Ala)(H_2O)] (**1**) and PS–[VO(fsal–L-Ile)(H_2O)] (**3**). Similarly, complexes PS–[Cu(fsal–D,L-Ala)(H_2O)] (**2**) and PS–[Cu(fsal–L-Ile)(H_2O)] (**4**) were isolated from the reaction of **III** and **IV** with $Cu(CH_3COO)_2$. The synthetic procedures, choosing fsal-L-Ile as an example, are represented by eqn (1) and (2).

$$\text{PS–H}_2\text{fsal–L-Ile} + \text{VOSO}_4 + 2\text{KOH} \rightarrow \text{PS–[VO(fsal–L-Ile)(H}_2\text{O)]} + \text{K}_2\text{SO}_4 + 2\text{H}_2\text{O} \quad (1)$$

$$\text{PS–H}_2\text{fsal–L-Ile} + \text{Cu(CH}_3\text{COO)}_2 \rightarrow \text{PS–[Cu(fsal–L-Ile)(H}_2\text{O)]} + 2\text{CH}_3\text{COOH} \quad (2)$$

The metal and ligand loading in the polymer-bound complexes presented in Table 1 suggest a ligand to metal loading stoichiometry of *ca.* 1 : 1 in all cases. This indicates that most of the immobilised ligand is involved in the coordination to the metal ion.

Similarly, the reaction of $VOSO_4$ and $Cu(CH_3COO)_2$ with equimolar amounts of ligands **I** and **II** in methanol/water yields the non-polymer bound complexes [VO(fsal–D,L-Ala)(H_2O)] (**5**), [Cu(fsal–D,L-Ala)(H_2O)] (**6**), [VO(fsal–L-Ile)(H_2O)] (**7**) and [Cu(fsal–L-Ile)(H_2O)] (**8**). The structures of similar complexes have been established and reported in the literature.[30–33] Scheme 3 presents the proposed structures of the anchored complexes, isolated and characterised by IR, UV-vis, EPR, elemental analysis, FE-SEM, EDAX and thermogravimetric studies.

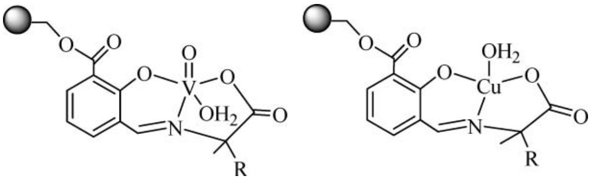

Scheme 3 Proposed structures for the polymer-anchored complexes: R = $-CH_3$ (D,L-Ala); R = $-CH(CH_2CH_3)CH_3$ (L-Ile).

Field emission scanning electron microscope and energy dispersive X-ray analysis studies

A comparative study using field emission scanning electron microscopy along with energy dispersive X-ray analysis was carried out taking single beads of pure chloromethylated polystyrene, polymer-anchored ligands and polymer-anchored metal complexes. As expected, the pure polymer beads have a smooth and flat surface and show two main components; carbon (80.7%) and chlorine (18.3%) on the surface, as evaluated semi-quantitatively by energy dispersive X-ray analysis. The introduction of a ligand onto the polystyrene beads through covalent bonding causes a light roughening of the top layer of beads. By EDAX analysis, considerable amounts of N and O, and a low amount of Cl (*ca.* 0.3%, see Table S1 of ESI†) were determined on the surface of the beads containing bound ligands. This indicates their nearly quantitative loading. Images of the metal complexes' polymer beads show further roughening of the top layer, which is probably due to the interaction of the metal ion with the ligand to accommodate the fixed geometry of the complex. EDAX analysis of these beads show a metal content along with C, N, O and Cl, suggesting the formation of metal complexes with the anchored ligand at various sites. The EDAX profiles of representative samples are presented in Fig. 1.

Thermogravimetric study

The thermal analyses of polymer-anchored metal complexes were carried out in an air atmosphere with a heating rate of 10 °C min^{-1}. The polymer-anchored metal complexes are generally thermally stable up to *ca.* 225 °C except for the small weight loss (*ca.* 2%) between 100–225 °C due to the loss of water. Thereafter, they decompose in several small fragments with exothermic weight losses at higher temperature. Both vanadium and copper based catalysts decompose in the temperature range of 225–500 °C. Quantitative measurement of weight losses at various

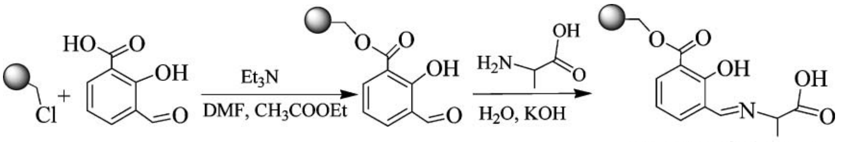

Scheme 2 Reaction scheme for the synthesis of polymer-bound complexes.

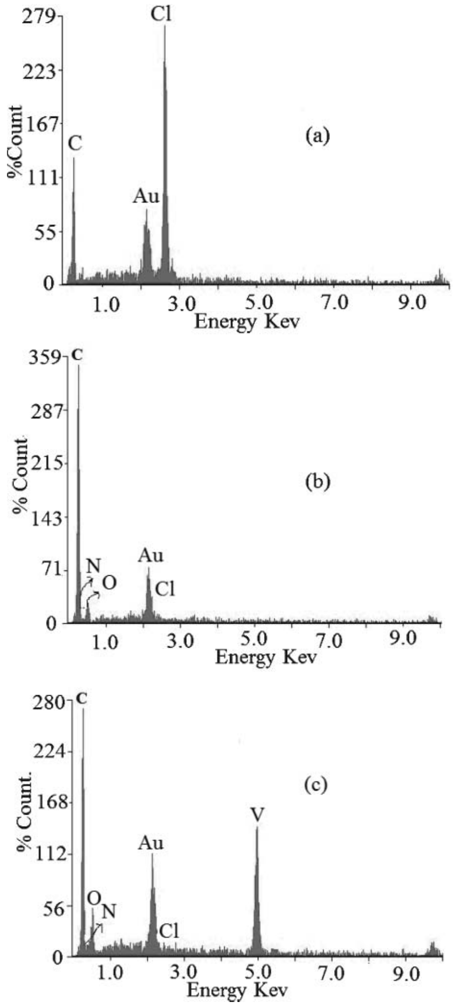

Fig. 1 EDAX profiles of (a) chloromethylated polystyrene, (b) PS–H_2fsal–D,L-Ala and (c) PS–[VO(fsal–D,L-Ala)(H_2O)].

stages was not possible due to the overlapping nature of the decompositions. However, the final residues of 5.2% (**1**), 6.7% (**2**) 5.0% (**3**) and 6.3% (**4**) suggest the formation of the respective metal oxides, CuO or V_2O_5.

IR spectral study

A partial list of IR spectral data for the ligands and the complexes are listed in Table S2 of the ESI.† The absence of characteristic strong bands that appear at 1264 and 673 cm^{-1} in chloromethylated polystyrene due to the CH_2Cl groups suggests the formation of an ester linkage by the reaction of chloromethyl group of styrene and the COOH group of 3-formylsalicyclic acid.[34] This is further supported by the appearance of a new band at 1674 cm^{-1} due to the ν(C=O); the free carboxylic group of 3-formylsalicylic acid exhibits ν(C=O) at 1663 cm^{-1}.[35] The IR spectra of the polymer-anchored ligands exhibit a sharp band at 1630 cm^{-1} due to ν(C=N) (azomethine group), and this band shifts to lower wavenumbers and appears at 1600–1608 cm^{-1}, suggesting the coordination of the azomethine nitrogen to the metal.[32,33] The coordination of the phenolic oxygen could not be ascertained unequivocally as the band at *ca.* 3400 cm^{-1} due to coordinated water interferes in this region. The complexes PS–[VO(fsal–D,L-Ala)(H_2O)] and PS–[VO(fsal–L-Ile)(H_2O)] exhibit sharp bands at 984 and 955 cm^{-1}, respectively, due to ν(V=O). The non-polymer bound vanadium and copper complexes display these spectral bands close to that of the anchored analogues.

Table 2 Electronic spectral data for the ligands and the complexes

Compounds	λ_{max}/nm^a
PS–H_2fsal–D,L-Ala	271, 241, 220
PS–[VO(fsal–D,L-Ala)·H_2O]	280, 221
PS–[Cu(fsal–D,L-Ala)·H_2O]	277, 236, 219
PS–H_2fsal–L-Ile	275, 241, 224
PS–[VO(fsal–L-Ile)·H_2O]	274, 239, 222
PS–[Cu(fsal–L-Ile)·H_2O]	277, 239, 224
[VO(fsal-D,L-Ala)·H_2O]	772(s), 543, 358, 301, 258, 236, 210
[Cu(fsal–D,L-Ala)·H_2O]	660(s), 356, 302, 254, 231, 209
[VO(fsal–L-Ile)·H_2O]	770(s), 530, 358, 303, 255, 237, 209
[Cu(fsal–L-Ile)·H_2O]	655(s), 304, 234, 209

^{a} s = shoulder band.

Electronic spectral study

The electronic spectra of the non-polymer-bound ligands and their complexes were recorded in methanol while that of the polymer-anchored ligands and their metal complexes were recorded in a nujol mull. These spectra are shown in Fig. S1, left (see ESI)† and the spectral data are presented in Table 2. Ligands **I** and **II** exhibit three spectral bands at 215, 240 and 275 nm in the UV region which are assigned to $\phi \rightarrow \phi^*$, $\pi \rightarrow \pi^*$ and $n \rightarrow \pi^*$ transitions, respectively. For the complexes, the first two bands shift towards lower wavenumbers, with two other bands appearing at *ca.* 255 and 300 nm in **5**, **6** and **7**. In addition, a new band of medium intensity appears at *ca.* 360 nm, which may be assigned either to a ligand to metal charge transfer band, or to a $\pi \rightarrow \pi^*$ transition originating mainly in the azomethine chromophore.[32] The expected d–d bands are observed only in methanolic solutions of higher concentrations of non-polymer bound complexes. The spectroscopic patterns shown by the polymer-anchored complexes (Fig. S1, right of ESI)† are essentially similar to those of the non-polymer-bound complexes, except for the broadness of the bands in nujol and only one band being observed for the $n \rightarrow \pi^*$ transition. The bands for lower energy (less intense) could not be observed in the polymer-anchored complexes due to their poor loading in the polymer matrix.

EPR studies

The EPR spectra for powdered samples of fresh and used polymer-anchored V(IV)O and Cu(II) complexes were recorded at room temperature. After swelling the polymer-anchored V(IV)O and Cu(II) complexes with DMF for *ca.* 1 h, these were 'frozen' in liquid nitrogen and their EPR spectra were also recorded and these powdered samples, in contact with the solvent, often give better-resolved EPR spectra, but in the present case no significant improvement in the resolution was obtained. Fig. 2 presents the EPR spectra for samples of PS–[VO(fsal–D,L-Ala)(X)] (**1**) (X = H_2O and/or DMF). The spectra recorded for PS–[VO(fsal–L-Ile)(X)] (**3**) (X = H_2O and/or DMF) are also similar. The EPR spectra of **1** and **3** are characteristic of magnetically diluted

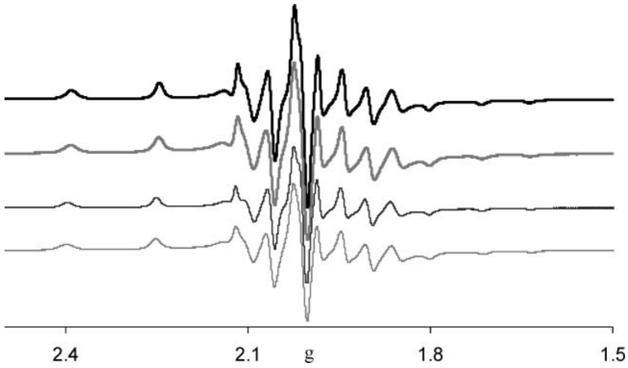

Fig. 2 Powder EPR spectra for samples of catalyst PS–[VO(fsal–D,L-Ala)(X)] **1**. Black (thick): **1** at room temperature; grey (thick): **1** after being used in the catalytic reaction, at room temperature; black (thin): **1** in contact with DMF at 77 K; grey (thin): **1** after being used in the catalytic reaction, in contact with DMF at 77 K.

V(IV)O complexes and the resolved EPR pattern indicates that the vanadium centres are well dispersed in the polymer matrix.

The spectra were simulated and the spin Hamiltonian parameters obtained[25] for the vanadium containing samples and are included in Table 3. All the EPR spectra are compatible with the expected binding mode (see Scheme 3), *i.e.* ($O^-{}_{Phe}$, N_{imine}, COO^-, H_2O or DMF)$_{equatorial}$, (H_2O or DMF)$_{axial}$, and with the EPR spectra recorded for similar complexes with *N*-salicylidene-aminoacidato ligands previously reported.[32,33] The slight differences in the several spectra recorded for **1**, and in the several spectra recorded for **3** may be explained by assuming small differences in the amount of H_2O or DMF coordinated to the V(IV)O centres. The EPR spectra for the powdered samples of **1** or **3** after being used for catalytic reactions (*e.g.* Fig. 2, grey spectra) show no significant differences from those of the fresh catalysts.

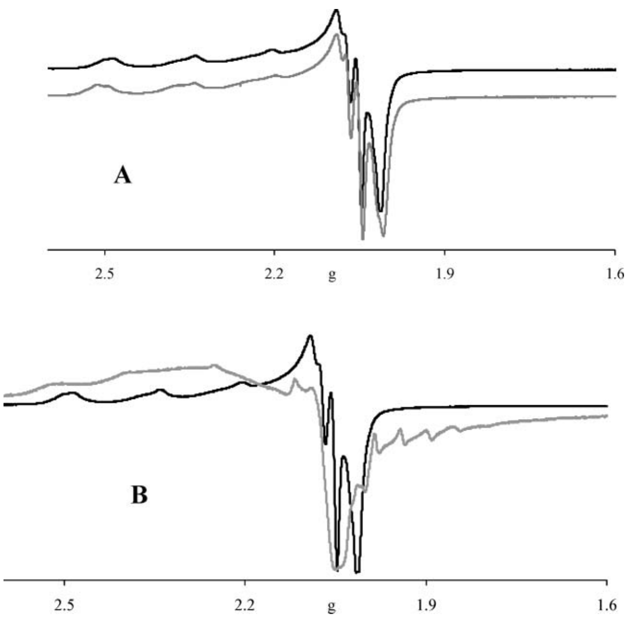

Fig. 3 EPR spectra for the powdered samples of the catalyst PS–[Cu(fsal–D,L-Ala)(X)] **2**. (A) Dry fresh catalyst at room temperature (black), and at 77 K for the powder in contact with DMF (grey); (B) dry fresh catalyst (black), and used dry catalyst (grey), both at room temperature.

Fig. 3A and Fig. 3B present EPR spectra for PS–[Cu(fsal–D,L-Ala)(X)] (**2**) (X = H_2O or DMF). Only slight differences are detected in the EPR spectra obtained at room temperature for powdered samples of the fresh polymer-anchored Cu(II) complexes **2** or **4** and those of the corresponding catalysts after swelling in DMF and freezing to 77 K (*e.g.* Fig. 3A). These differences may be explained by assuming small changes in the relative amount of H_2O and DMF coordinated to the Cu centres. At least two distinct species are detected in each of the EPR spectra recorded and Table S3, in the ESI,† includes the spin Hamiltonian parameters calculated by simulation of the spectra. Although the values obtained for the distinct species present in the fresh catalysts are not very accurate, globally the EPR spectra are consistent with a NO_3 binding mode with some, but normally not very significant distortion from a square planar arrangement of the donor atoms.

However, the EPR spectra of catalysts **2** and **4** after being used in the catalytic reactions (*e.g.* grey curve in Fig. 3B) show significant differences from the fresh catalysts, and at least 3 distinct species are detected. In fact, weak features for $g \approx 1.8$–1.6 indicate the

Table 3 Spin Hamiltonian parameters obtained from the experimental EPR spectra recorded for powdered samples of **1** and **3**, and of the corresponding non-polymer-bound complexes **5** and **7** dissolved in DMF

Catalyst	Sample	$g_\parallel$	$A_\parallel/\times10^{-4}$ cm^{-1}	$g_\perp$	$A_\perp/\times10^{-4}$ cm^{-1}
[VO(fsal–D,L-Ala)(X)], **5**	In DMF	—	—	—	—
1st species	—	1.948	169.4	1.980	61.4
2nd species[a]	—	1.947	171.1	1.980	61.4
PS–[VO(fsal–D,L-Ala)(X)], **1**	Fresh	1.943	168.7	1.978	60.1
PS–[VO(fsal–D,L-Ala)(X)], **1**	Used	1.943	169.5	1.978	60.8
PS–[VO(fsal–D,L-Ala)(X)], **1**–DMF[b]	Fresh	1.944	170.2	1.979	59.1
PS–[VO(fsal–D,L-Ala)(X)], **1**–DMF[b]	Used	1.943	170.8	1.979	60.0
[VO(fsal–L-Ile)(X)], **7**	In DMF	—	—	—	—
1st species	—	1.947	168.6	1.980	61.8
2nd species[a]	—	1.947	171.3	1.980	61.3
PS–[VO(fsal–L-Ile)(X)], **3**	Fresh	1.944	168.6	1.978	60.0
PS–[VO(fsal–L-Ile)(X)], **3**	Used	1.943	168.7	1.978	61.6
PS–[VO(fsal–L-Ile)(X)], **3**–DMF[b]	Fresh	1.945	170.1	1.974	59.2
PS–[VO(fsal–L-Ile)(X)], **3**–DMF[b]	Used	1.944	170.4	1.979	59.8

[a] The spin Hamiltonian parameters of the two species are very close, possibly they are isomeric species. [b] Spectrum recorded after swelling the solid in DMF.

presence of a dimeric complex; the corresponding features that should appear at $g \approx 2.4$–2.6 cannot be seen because of the broad bands due to the presence of at least two monomeric complexes and of some dipolar interactions operating. The features observed at $g \approx 1.90 \pm 0.05$ probably correspond to the g_x components of a highly distorted monomeric Cu complex, whose g_z components are at $g \approx 2.4 \pm 0.1$.[36] A second monomeric complex with $g_z \approx 2.05$ is also present but the corresponding $A_\parallel$ values cannot be estimated due the unresolved pattern of the $g \approx 2.6$–2.2 region of the spectra for catalysts **2** and **4** after being used for the catalytic reactions.

Catalytic activity

Oxidation of *p*-chlorotoluene. The oxidation of *p*-chlorotoluene by aqueous H_2O_2 as the oxidant was studied using the polymer-bound catalysts. The reaction gave five oxidation products namely, *p*-chlorobenzaldehyde, *p*-chlorobenzyl alcohol, 3-methyl-6-chlorophenol, 2-methyl-5-chlorophenol and *p*-chlorobenzoic acid (see Scheme 4). Among the catalysts studied, PS–[Cu(fsal–D,L-Ala)(H_2O)] was taken as a representative one and different parameters *e.g.* amount of oxidant, catalyst and temperature were studied to optimise the reaction conditions to achieve maximum oxidation of *p*-chlorotoluene to *p*-chlorobenzaldehyde.

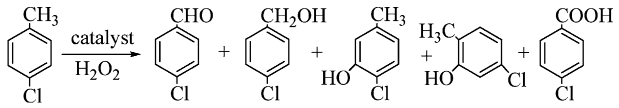

Scheme 4

The effect of H_2O_2 concentration on the oxidation of *p*-chlorotoluene is illustrated in Fig. 4A. A conversion of *ca.* 8.7% was achieved at a *p*-chlorotoluene to aqueous H_2O_2 molar ratio of 1 : 1 in 6 h when *p*-chlorotoluene (1.26 g, 0.010 mol), 30% H_2O_2 (2.27 g, 0.020 mol) and PS–[Cu(fsal–D,L-Ala)(H_2O)] (0.025 g) were placed in acetonitrile (20 mL) and reacted at 80 °C. This conversion improved to *ca.* 10% on increasing the ratio to 1 : 3 and to *ca.* 15.4% at a *p*-chlorotoluene to H_2O_2 molar ratio of 1 : 4. These results indicated a linear increment in conversion upon increasing the H_2O_2 concentration. However, the selectivity of *p*-chlorobenzaldehyde decreases at higher concentration of oxidant due to its further oxidation to *p*-chlorobenzoic acid. No further increment in the oxidation of *p*-chlorotoluene was observed beyond a 6 h contact time.

Similarly three different amounts of catalyst *viz.* 0.025, 0.035 and 0.050 g were taken at fixed reaction conditions for *p*-chlorotoluene (1.26 g, 0.010 mol), H_2O_2 (2.27 g, 0.020 mol), CH_3CN (20 mL) and temperature (80 °C) to understand the effect of the relative amount of catalyst on the reaction. As shown in Fig. 4B, 0.025 g of catalyst is adequate and any further increment in the amount of catalyst had no affect on the conversion under the above conditions.

The temperature of the reaction has an influence on the oxidation of *p*-chlorotoluene. As illustrated in Fig. 4C, 80 °C was the most favorable temperature under the above reaction conditions to obtain the maximum conversion of *p*-chlorotoluene. The conversion increases with the temperature.

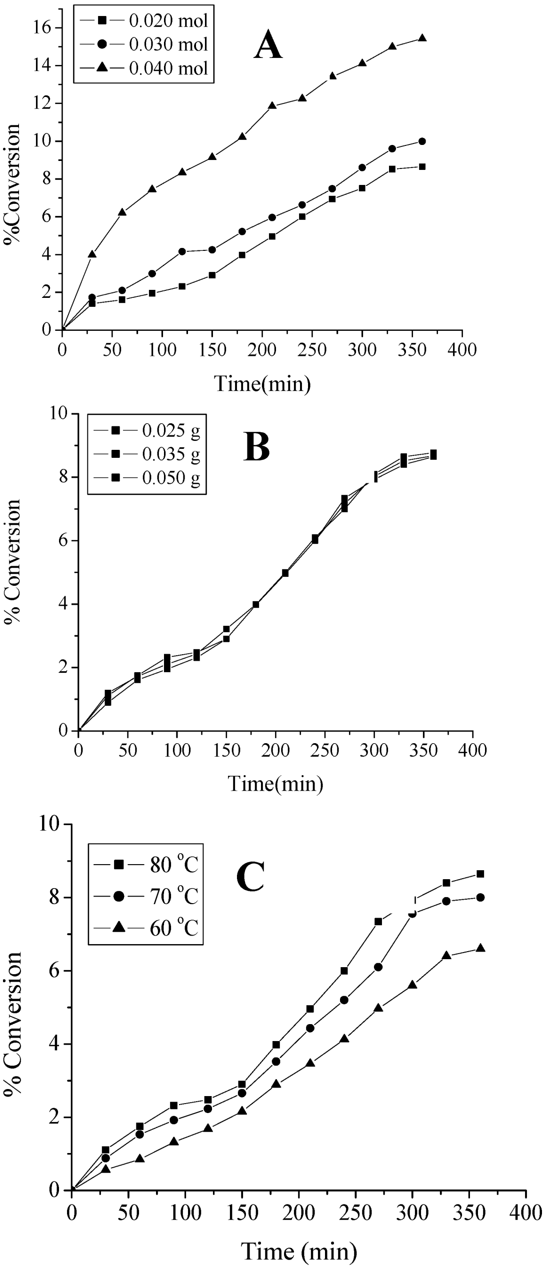

Fig. 4 Oxidation of *p*-chlorotoluene. (A) Effect of the H_2O_2 concentration: reaction conditions; PS–[Cu(fsal–D,L-Ala)(H_2O)] (0.025 g), *p*-chlorotoluene (1.26 g, 0.010 mol), acetonitrile (20 mL) and 80 °C. (B) Effect of the relative amount of catalyst: reaction conditions; *p*-chlorotoluene (1.26 g, 0.010 mol), 30% H_2O_2 (2.27 g, 0.020 mol), acetonitrile (20 mL) and 80 °C. (C) Effect of temperature: reaction conditions; PS–[Cu(fsal–D,L-Ala)(H_2O)] (0.025 g), *p*-chlorotoluene (1.26 g, 0.010 mol), 30% H_2O_2 (2.27 g, 0.020 mol) and acetonitrile (20 mL).

Therefore, from these experiments, for the maximum oxidation of 0.010 mol of *p*-chlorotoluene the best conditions are: catalyst (0.025 g), aqueous 30% H_2O_2 (2.27 g, 0.020 mol), CH_3CN (20 mL) and temperature (80 °C). The other polymer-bound catalysts were also tested, using these experimental conditions, and the corresponding results are presented in Table 4.

From the results presented in Table 4 it is clear that the conversion of *p*-chlorotoluene follows the order: PS–[VO(fsal–D,L-Ala)(H_2O)] (13.8%) > PS–[VO(fsal–L-Ile)(H_2O)] (12.4%) > PS–[Cu(fsal–L-Ile)(H_2O)] (8.8) > PS–[Cu(fsal–D,L-Ala)(H_2O)] (8.7%).

Table 4 Conversion of *p*-chlorotoluene and selectivity of various products after 6 h of reaction time[a]

Catalyst	%Conv.	TOF/h^{-1}	%Selectivity 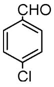	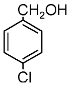	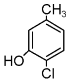	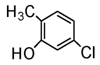	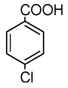
PS–[VO(fsal–D,L-Ala)(H_2O)]	13.8	8.68	62.8	14.2	4.9	6.8	11.3
PS–[VO(fsal–D,L-Ala)(H_2O)][b]	13.3	—	62.5	14.2	4.8	7.0	11.5
PS–[Cu(fsal–D,L-Ala)(H_2O)]	8.7	5.62	15.6	32.4	7.7	24.0	20.3
PS–[Cu(fsal–D,L-Ala)(H_2O)][b]	8.0	—	15.8	32.3	7.7	24.1	20.1
PS–[VO(fsal–L-Ile)(H_2O)]	12.4	9.25	54.5	13.5	9.3	10.4	12.3
PS–[VO(fsal–L-Ile)(H_2O)][b]	12.0	—	54.4	13.2	9.6	10.4	12.4
PS–[Cu(fsal–L-Ile)(H_2O)]	8.8	6.07	15.9	27.6	7.2	26.7	22.7
PS–[Cu(fsal–L-Ile)(H_2O)][b]	8.2	—	16.0	27.4	7.0	27.0	22.6
[VO(fsal–D,L-Ala)(H_2O)]	8.3	5.20	61.1	12.5	7.6	8.8	9.9
[Cu(fsal–D,L-Ala)(H_2O)]	6.8	4.46	16.0	23.2	13.2	22.2	25.0
[VO(fsal–L-Ile)(H_2O)]	8.0	5.97	59.7	15.4	6.4	8.3	10.3
[Cu(fsal–L-Ile)(H_2O)]	7.0	4.81	16.2	24.9	12.4	22.9	23.5

[a] Reaction conditions: *p*-chlorotoluene (0.010 mol), 30% H_2O_2 (0.020 mol), catalyst (0.025 g), CH_3CN (20 mL) and temperature, 80 °C. [b] First cycle of used catalyst.

Thus, the vanadium based catalysts are better than the copper based catalysts. However, within each of the particular metal systems both complexes present nearly equal catalytic potential. The selectivity for the different reaction products also differs: for the vanadium based polymer-anchored complexes, the selectivity of the various products follows the order: *p*-chlorobenzaldehyde >> *p*-chlorobenzyl alcohol > *p*-chlorobenzoic acid > 2-methyl-5-chlorophenol > 3-methyl-6-chlorophenol, while for the polymer-bound copper complexes the order is: *p*-chlorobenzyl alcohol > 2-methyl-5-chlorophenol > *p*-chlorobenzoic acid > *p*-chlorobenzaldehyde > 3-methyl-6-chlorophenol.

The used catalysts were washed with acetonitrile, dried at 100 °C and tested for their catalytic activities. The corresponding data is also presented in Table 5 and show that there is not much loss in catalytic activity. The non-polymer-bound complexes exhibit lower conversions as well as lower turn-over frequencies.

Oxidation of cyclohexene. The oxidation of cyclohexene catalysed by polymer-anchored complexes gave cyclohexene epoxide, 2-cyclohexene-1-ol, 2-cyclohexene-1-one and cyclohexane-1,2-diol as shown in Scheme 5.

Both H_2O_2 and TBHP are known to oxidise cyclohexene in the presence of alumina-supported metal complexes. However, under similar conditions H_2O_2 gave much better epoxidation results for cyclohexene than TBHP. TBHP as an oxidant promotes the allylic oxidation pathway, and epoxidation products only form in low amounts, while with the use of H_2O_2 the oxidation occurs mainly on the double bond and cyclohexene epoxide is obtained almost as the sole product. The formation of the allylic oxidation products 2-cyclohexene-1-one and 2-cyclohexene-1-ol reflects the preferential attack of the activated C–H bond over the C=C bond.[37] Valentine and co-workers have suggested that the species responsible for the cyclohexene oxidation is the product formed from the cleavage of

Table 5 Conversion of cyclohexene and selectivity of the various oxidation products after 6 h of reaction time

Catalyst	%Conv.	TOF/h^{-1}	%Selectivity 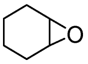	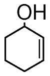	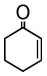	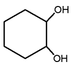
PS–[VO(fsal–D,L-Ala)(H_2O)]	78.8	49.6	34.7	48.1	6.8	10.4
PS–[VO(fsal–D,L-Ala)(H_2O)][a]	78.0	—	34.6	48.3	6.7	10.4
PS–[Cu(fsal–D,L-Ala)(H_2O)]	32.5	21.3	39.3	53.1	4.3	3.3
PS–[Cu(fsal–D,L-Ala)(H_2O)][a]	31.6	—	38.8	53.5	4.3	3.4
PS–[VO(fsal–L-Ile)(H_2O)]	76.6	57.1	36.1	44.7	8.2	11.0
PS–[VO(fsal–L-Ile)(H_2O)][a]	76.0	—	36.3	44.6	8.2	10.9
PS–[Cu(fsal–L-Ile)(H_2O)]	29.4	20.2	42.3	45.7	3.6	8.4
PS–[Cu(fsal–L-Ile)(H_2O)][a]	28.2	—	41.9	46.0	3.6	8.5
[VO(fsal–D,L-Ala)(H_2O)]	53.8	33.9	38.9	52.6	5.1	3.4
[Cu(fsal–D,L-Ala)(H_2O)]	26.3	17.3	36.2	49.6	9.7	4.5
[VO(fsal–L-Ile)(H_2O)]	50.5	37.7	40.0	48.4	6.3	5.28
[Cu(fsal–L-Ile)(H_2O)]	18.1	12.4	39.7	42.1	8.3	9.9

[a] First cycle of used catalyst.

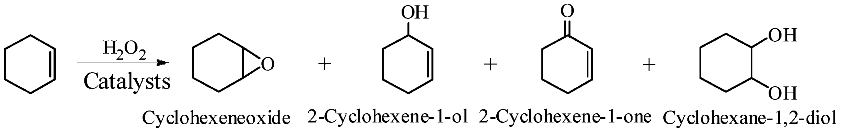

Scheme 5

the O–O bond, whereas epoxidation occurs *via* the direct reaction of the olefin with the coordinated HOO^-. Since the O–O bond of HOOH is 5 kcal mol^{-1} stronger than TBHP, an HOO^- complex is expected to have a higher activation energy for O–O bond cleavage than a TBHP complex and therefore, will have a longer lifetime[38] and a higher probability of forming the epoxide.

We have optimised different parameters such as the amount of oxidant, catalyst, solvent and temperature of the reaction mixture for the maximum oxidation of cyclohexene while considering PS–[VO(fsal–D,L-Ala)(H_2O)] as the representative catalyst. Three different cyclohexene to aqueous 30% H_2O_2 molar ratios *viz.* 1 : 1, 1 : 2 and 1 : 3 were considered at a fixed amount of cyclohexene (0.082 g, 0.010 mol), PS–[VO(fsal–D,L-Ala)(H_2O)] (0.025 g) and acetonitrile (20 mL), with the reaction being carried out at 70 °C. A maximum of 22.9% conversion was achieved at a cyclohexene to H_2O_2 molar ratio of 1 : 1. Increasing this ratio to 1 : 2 increased the conversion to 70.4% while a 1 : 3 molar ratio gave 75.2% conversion (Fig. 5A). Analysis of the effect of substrate to oxidant ratios suggests that increasing the amount of oxidant decreases the formation of cyclohexene oxide whilst increasing the formation of 2-cyclohexene-1-ol and cyclohexane-1,2-diol slightly. Further increments in the oxidant amount has not resulted in any significant change in conversion, which suggests that a large amount of oxidant is not an essential condition to improve the oxidation of cyclohexene. Therefore, a cyclohexene to H_2O_2 molar ratio of 1 : 2 was considered to be adequate in obtaining the highest cyclohexene conversion (*ca.* 70%).

Using (0.082 g, 0.010 mol) of cyclohexene, 30% H_2O_2 (2.27 g, 0.020 mol) and acetonitrile (20 mL), three different amounts of catalyst *viz.* 0.015, 0.025 and 0.035 g were considered for the oxidation of cyclohexene and the reaction was monitored at 70 °C. The results obtained as a function of time, presented in Fig. 5B, indicate that 0.035 g of catalyst yields a maximum conversion of *ca.* 75%, while 0.025 and 0.015 g of catalyst gave *ca.* 70 and 63% conversion, respectively in 6 h of reaction time. Further increments in the amount of catalyst showed no significant change in the conversion.

Fig. 5C illustrates the effect of temperature on the oxidation of cyclohexene as a function of time under the above optimised reaction conditions. From the figure we conclude that 80 °C is the best suited temperature for the conversion of cyclohexene. At this temperature, a maximum of *ca.* 79% conversion of cyclohexene was achieved in 6 h of contact time. At lower temperature, *viz.* 60 and 70 °C, the conversions obtained were *ca.* 56 and 70%, respectively.

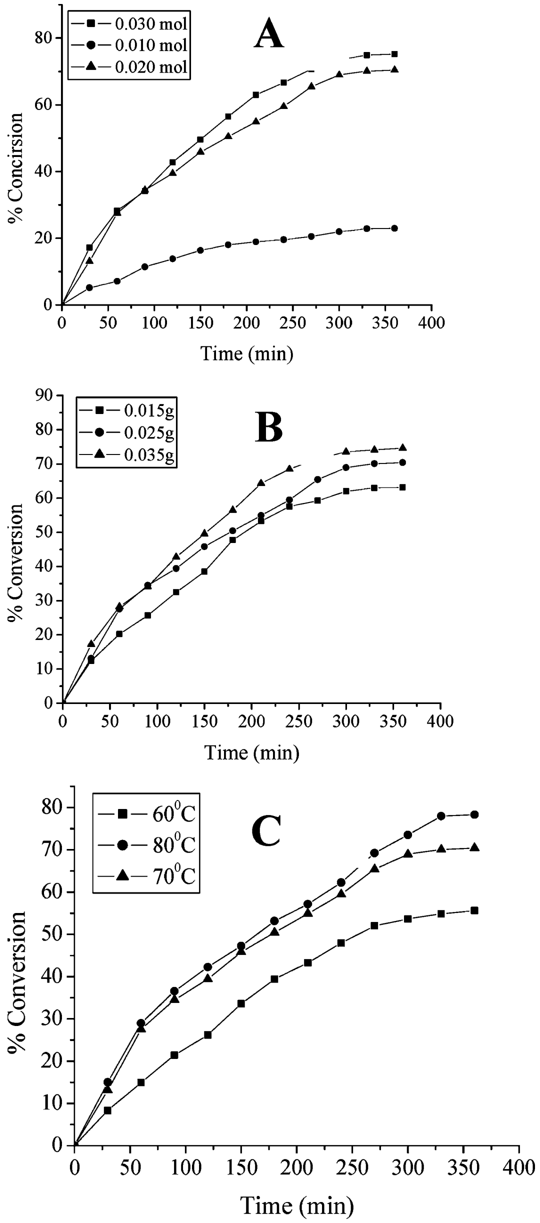

Fig. 5 Oxidation of cyclohexene. (A) Effect of H_2O_2: reaction conditions; cyclohexene (0.082 g, 0.010 mol), PS–[VO(fsal–D,L-Ala)(H_2O)] (0.025 g), acetonitrile (20 mL) and 70 °C. (B) Effect of amount of catalyst: reaction conditions; cyclohexene (0.082 g, 0.010 mol), 30% H_2O_2 (2.27 g, 0.020 mol), acetonitrile (20 mL) and 70 °C. (C) Effect of temperature: reaction conditions; cyclohexene (0.082 g, 0.010 mol), PS–[VO(fsal–D,L-Ala)(H_2O)] (0.025 g), 30% H_2O_2 (2.27 g, 0.020 mol) and acetonitrile (20 mL).

Therefore, under the optimised conditions *i.e.* cyclohexene (0.82 g, 0.010 mol), H_2O_2 (2.27 g, 0.020 mol), catalyst (0.025 g) CH_3CN (20 mL) and temperature (80 °C), the performance of the other catalysts was also studied and the conversions after 6 h of reaction time and the product selectivity are presented in Table 5. It is clear from the table that the vanadium based polymer-anchored catalysts are better than the copper based ones for the oxidation of cyclohexene, and within each metal system the catalytic performances are quite similar. The selectivity of the products follows the order: 2-cyclohexene-1-ol > cyclohexene oxide > cyclohexane-1,2-diol > 2-cyclohexene-1-one.

The catalytic activity of the used catalysts, after washing with acetonitrile and drying at 100 °C, was also tested and the corresponding data are presented in Table 5. These results indicate that the catalytic activity of the used catalysts is similar to that of the fresh ones. However, non-polymer bound complexes exhibit lower conversions along with lower turn-over frequencies (Table 5), but the selectivity for the major products, 2-cyclohexene-1-ol and cyclohexene oxide, is the same.

Considerations about the reaction mechanism and intermediate species

Peroxo-complexes may be able to transfer oxygen to aromatic hydrocarbons. However, alkanes are much less readily hydroxylated than aromatic hydrocarbons, and mixtures of alcohols and ketones are formed. The mechanism of oxygen transfer of peroxo–metal complexes to nucleophilic substrates has been a matter of considerable debate, and overall two main alternatives have been proposed. One proceeds through a simple bimolecular mechanism involving the nucleophile and the peroxo–metal complex. The other is a mechanism that involves the formation of an intermediate resulting from the coordination of the substrate to the metal.

It is known that [V(IV)O(sal–Am)(X)]-type complexes (Am = amino acid with non-coordinating side chains, X = H_2O, MeOH) oxidise easily; namely [V(IV)O(sal–L-Ala)(H_2O)] upon oxidation in methanol forms [V(V)O(sal–L-Ala)(MeO)(MeOH)].[39] Vanadium(V) complexes are also known to form oxoperoxovanadium(V) complexes in the presence of excess H_2O_2.[2,39–41]

In the absorption spectrum, the complex [V(V)O(sal–L-Ala)(MeO)(MeOH)] has λ_{max} at ~360 and 500 nm,[39] due to $\pi \rightarrow \pi^*$ (azomethine, see above) and charge-transfer transitions, respectively, and upon addition of *t*-butyl-hydroperoxide a relatively intense band appears at *ca.* 450 nm. [V(V)O(sal–L-Val)(MeO)(MeOH)] in methanol also presents[42] bands at *ca.* 420 nm (CT), and the corresponding V(IV)O complex a d–d band at *ca.* 700 nm.[33]

To get information on the reaction pathway and the intermediate species formed during the oxidation of the substrates, a methanolic solution of the non-polymer-bound complex **5** was treated with a MeOH solution of H_2O_2, and the progress of the reaction was monitored by UV-vis. Fig. 6 presents the spectral changes observed. Thus, the addition of one-drop portions of H_2O_2 to a *ca.* 10^{-4} M solution of [VO(fsal–D,L-Ala)(H_2O)] in MeOH resulted in only a slight reduction of the intensity of the band appearing at 356 nm, along with the gradual appearance of a new band at *ca.* 410–420 nm. The bands appearing at 249 nm were slowly converted into weak shoulders that then increased in intensity, while the intensity of the 238 nm bands increased. The intensity of the 208 nm band also increases. At higher concentration (*ca.* 10^{-3} M) [VO(sal–D,L-Ala)(H_2O)] **5** also exhibits two bands at 543 and 772 nm, as shown in the inset of Fig. 6. Upon addition of H_2O_2 the bands appearing at ~772 nm slowly flatten, while the intensity of the 543 nm band is progressively increased with broadening and finally disappeared.

We interpret these results as due to the formation of [V^{V}O(fsal–D,L-Ala) (MeO)(MeOH)] (**9**) and of an oxoperoxovanadium(V) species. Similar spectral changes have been reported for [VO(fsal–β-Ala)(H_2O)] (H_2fsal–β-Ala = a Schiff base derived from 3-formylsalicylic acid and β-alanine) upon treatment with H_2O_2.[13] The band appearing at *ca.* 410–420 nm is probably due to a LMCT band of the monoperoxo complex[39,40,43,44] but is probably superimposed with the CT transition from the phenolate group at about the same energy (or slightly lower), as observed in [V^{V}O(sal–L-Am)(MeO)(MeOH)] complexes.[33]

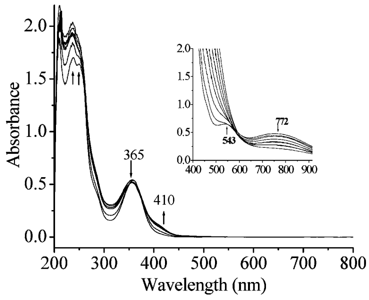

Fig. 6 Titration of [V^{IV}O(fsal–D,L-Ala)(H_2O)] **5** with H_2O_2. The spectra were recorded after successive additions of one-drop portions of H_2O_2 (1 mL of 30% H_2O_2 dissolved in 10 mL of methanol) to 10 mL of *ca.* 10^{-4} M methanolic solution of [VO(fsal–D,L-Ala)(H_2O)]. The inset shows equivalent titrations, but with higher concentrations of a [VO(fsal–D,L-Ala)(H_2O)] solution (*ca.* 10^{-3} M).

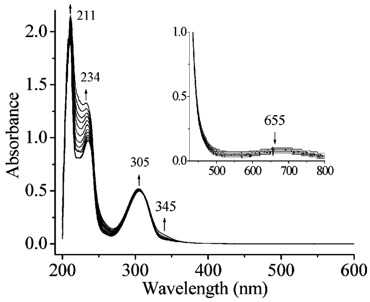

Fig. 7 Titration of [Cu(fsal–L-Ile)(H_2O)] (**8**) with H_2O_2. The spectra were recorded after the successive additions of one drop portions of H_2O_2 (1 mL of 30% H_2O_2 dissolved in 10 mL of methanol) to 10 mL of *ca.* 10^{-4} M methanolic solution of [Cu(fsal–L-Ile)(H_2O)]. The inset shows equivalent titrations, but with higher concentrations of a [Cu(fsal–L-Ile)(H_2O)] solution (*ca.* 10^{-3} M).

The ^{51}V NMR spectrum of a 4 mM solution of V^{IV}O(fsal–D,L-Ala)(X) **5** (in 80% MeOH and 20% MeOD), upon standing in contact with air for *ca.* 7 days, shows one peak at −553 ppm and two close, equally intense peaks at −562 and −566 ppm. We assign these two latter peaks to the stereoisomers that may form for [V^{V}O(fsal–D,L-Ala)(MeO)(MeOH)] **9**. For [V^{V}O(naph–L-Phe)(1,3-butO)(1,3-butOH)] (naph-L-Phe = *N*-(2-oxidonaphthal)–Phe–O$^-$ and 1,3-butOH = 1,3-butanediol) four peaks in the range −553 to −585 ppm have been reported in the ^{51}V NMR spectra,[45] and in the case of [V^{V}O(naph–L-Ala)(Bu^{S}O)(Bu^{S}OH)] (Bu^{S}OH = D,L-*sec*-butyl alcohol) three peaks were found in the range −583 to −590 ppm and were also assigned to the stereoisomers of the Schiff base V(V) complexes.[46] The peak at *ca.* −553 ppm possibly corresponds to VO_2^+ (V_1), indicating some significant hydrolysis of the V(V) complexes after one week of contact of the solution with air (Table S4, ESI).†

Upon progressive addition of H_2O_2 to this oxidised solution of **5**, the relative intensities of the peaks change: the −553 ppm peak decreases its relative intensity, and after 8 equiv. of H_2O_2 it is no longer detected, while a peak at −581 ppm increases its relative intensity. This latter peak may be assigned to the formation of $[V^{V}O(fsal–D,L\text{-}Ala)(O_2)(MeOH)]^-$ (see Table S4, ESI).† Overall these ^{51}V NMR spectra confirm the results and interpretation of Fig. 6.

After 9 equiv. of H_2O_2 have been added to this oxidised solution of **5**, styrene (used here as a model of an alkene) was progressively added to this mixture, namely a total of 2, 3, 5, 8, 10, 15, 18, 22, 30, 35, 40, and 45 equiv. of styrene were added and the corresponding ^{51}V NMR spectra were recorded (see Table S4, ESI).† No new peaks were detected but the global intensity of the ^{51}V NMR spectra progressively decreased upon addition of styrene. For the solutions where 40 or 45 equiv. of styrene have been added almost no ^{51}V NMR signal was detected. Therefore, upon addition of styrene the oxidation of this substrate occurred, with the concomitant reduction of all V(V) species present.

In a distinct experiment, to a 4 mM solution of $[V^{IV}O(fsal–D,L\text{-}Ala)(X)]$ **5** (in 80% MeOH and 20% MeOD), which was kept overnight in contact with air, 1 equiv. of H_2O_2 was added. The ^{51}V NMR spectrum of this solution showed peaks at −553, −562 and −566 ppm. Upon addition of amounts of styrene (dissolved in methanol) no new peaks were detected, but the intensity of all peaks decreased as styrene was added.

The oxoperoxovanadium(V) species actively participates in the oxidation by transferring one of its peroxo oxygens to the substrate. Whether the mechanism involves an intermediate complex with coordination of styrene, followed by an alkylperoxo species, then yielding the products, or proceeds without the intermediate binding of the substrate, is not clear. In fact, the EPR spectra of the 4 mM methanolic solutions of $[V^{IV}O(fsal–L\text{-}Ile)(H_2O)]$ **7**, did not change much after progressive addition of styrene (*ca.* 2 to 10 equiv.). After 10 equiv. of styrene had been added, the pattern of the spectrum was very similar to that of **7**, but the spin Hamiltonian parameters had slightly changed (from $g_\parallel = 1.946$, $g_\perp = 1.980$, $A_\parallel = 172.0$ and $A_\perp = 62.4 \times 10^{-4}$ cm^{-1} for **7** in MeOH, to $g_\parallel = 1.946$, $g_\perp = 1.980$, $A_\parallel = 171.5$ and $A_\perp = 61.9 \times 10^{-4}$ cm^{-1} for **7** + 10 equiv. of styrene). Although for other systems we had clear evidence for the binding of styrene to the V(IV) centre,[47] here the evidence for the coordination of styrene is weak. Addition of different amounts of H_2O_2 (1, 2, 3, 5, 7 equiv.) to this solution of **7** containing 10 equiv. of styrene also did not change the pattern of the EPR spectra, but its intensity decreased and after the addition of 7 equiv. of H_2O_2 the EPR signal was almost zero. The $A_\parallel$ values apparently showed a very small decrease, but as the intensity of the spectra decreased this cannot be clearly stated or associated to the binding of a peroxo, hydroperoxide or peroxy species.

Progressive additions of different amounts of H_2O_2 (2, 4, 5 equiv.) to a 4 mM methanolic solution of **7** also did not change the EPR signal, but decreased its intensity.

The EPR spectra of 4 mM methanolic solutions of $[Cu(fsal–L\text{-}Ile)(H_2O)]$ **8**, showed no change upon the progressive addition of styrene (1, 3, 5, 8, 10 equiv.). After 10 equiv. of styrene had been added, the pattern of the spectrum was identical to that of **8**, and there was no indication to support the coordination of styrene to the Cu centre. Addition of different amounts of H_2O_2 (2 to 10 equiv.) to the solution of **8** containing 10 equiv. of styrene also did not change the pattern of the EPR spectra.

The addition of a methanolic solution of H_2O_2 to 10 mL of a *ca.* 10^{-3} M methanolic solution of $[Cu(fsal–L\text{-}Ile)(H_2O)]$ **8** resulted in the reduction in the intensity of the d–d band at 655 nm without changing its position, but further addition of H_2O_2 did not reduce its intensity further (inset of Fig. 7). The addition of H_2O_2 to a dilute solution of **8** (*ca.* 10^{-4} M) caused only slight increments in the intensities of the 211 and 305 nm bands without changing their position, while a considerable increase in the band maximum was observed in the 234 nm band (Fig. 7). A weak shoulder also appeared at 345 nm. These changes in the UV-vis spectra indicate the interaction of the peroxo group with the Cu(II) centre in the complex.

At least three types of peroxo species *viz.* side-on Cu(II)–(μ-η^2-peroxo)–Cu(II), bis(μ-oxo-Cu(III)) and Cu(II)–O–O–H (copper hydroperoxide) have been reported in the literature during catalytic actions.[48] As copper complexes supported on polymers are expected to be monomeric, and they all have one weakly coordinated ligand (water) with exchangeable properties, the formation of [(HOO)–Cu(II)–(fsal–D,L-Am)] as an intermediate species may be expected upon interaction with H_2O_2. These intermediates are expected to transfer the oxygen atoms to the substrates to give the products. The presence of a weak, broad band at *ca.* 655 nm even after H_2O_2 addition is possibly due to charge transfer due to Cu hydroperoxide complex formation.[49]

A possible mechanism, following what was outlined by Mimoun *et al.*,[50] involves the formation of a V(V)-oxoperoxo complex, which upon coordination of the substrate, and insertion of the bound alkene into one of the metal–peroxo bonds, followed by the collapse of the resulting peroxometallocycle yields the epoxide. However, no data was obtained to support the coordination of the arene. A bimolecular mechanism involving the nucleophilic attack of the substrate at the protonated peroxide ligand is also possible.

With the Cu(II) complexes the formation of peroxo or hydroperoxo species is not so favourable and the conversions are lower than with the vanadium complexes. The redox reactions involving Cu(II)/Cu(III) species are also not so easy as with the V(IV)/V(V) complexes. Therefore, the mechanism possibly involves the nucleophilic attack of the substrate at the protonated peroxide ligand, L-Cu(II)–OOH being the active catalyst.

The mechanism of the oxidation of alkanes and alcohols is normally considered consistent with single transfer steps.[2] For the vanadium complexes the formation of an oxoperoxovanadium(V) is usually assumed. For hydroxylation of benzene either: (i) a mechanism in which the oxoperoxovanadium(V) undergoes intramolecular electron transfer to give a $V(IV)–(O_2^{\bullet-})$ biradical, which inserts into aromatic or aliphatic C–H bonds[1] or (ii) the reaction occurs *via* the radical anion of the vanadium(V) complex.[51] Other authors have also reported radical mechanisms involving alkylhydroperoxide intermediates for oxidation of alkanes, alkenes and arenes.[52]

Recyclability and heterogeneity of the reaction

The used catalysts PS–[VO(fsal–D,L-Ala)(H_2O)] and PS–[Cu(fsal–D,L-Ala)(H_2O)], after separating from the reaction mixture, washing with acetonitrile and drying at *ca.* 120 °C, were further applied for catalytic reactions under similar conditions in both cases. No significant loss in the activity occurred, though the EPR study suggests a slight modification in the coordinating mode of the copper-based catalysts after use. The filtrate collected after each catalytic reaction was placed further into the reaction flask and the reaction was continued at the optimised conditions for 3 h after adding fresh oxidant. The gas chromatographic analysis of the reaction mixture showed no increase in the conversion. This confirms that the reaction did not proceed upon the removal of the solid catalyst and hence the reaction was heterogeneous in nature. In addition, the filtrates tested by ICP-MS for all catalysts for the presence of any leached metal ions showed negative results.

The non-polymer bound complexes are considerably less efficient than their polymer-bound counterparts. We expect this to be due mainly to a global concentration effect, as the non-polymer bound complexes partially decompose in solution due to hydrolysis of the ligand and oxidation of V(IV). In contrast, the polymer-bound complexes are stable towards decomposition and hydrolysis.

Conclusions

Polymer-anchored oxovanadium(IV) and copper(II) complexes of ligands derived from 3-formylsalicyclic acid and D,L-alanine or L-isoleucine have been prepared and characterised. These complexes were used with success as catalysts for the oxidation of *p*-chlorotoluene and cyclohexene. The reaction conditions were optimised to obtain maximum oxidation products. Under the optimised conditions, *p*-chlorotoluene gave four products having a selectivity order of: *p*-chlorobenzaldehyde >> *p*-chlorobenzylalcohol > *p*-chlorobenzoic acid > 2-methyl-5-chlorophenol > 3-methyl-6-chlorophenol. The oxidation of cyclohexene also gave four products with a selectivity order of: 2-cyclohexene-1-ol > cyclohexene oxide > cyclohexane-1,2-diol > 2-cyclohexene-1-one. The corresponding non-polymer bound complexes have also been prepared and their catalytic activities evaluated. The oxidation of the substrates proceeds through either a peroxooxovanadium(V) or hydroperoxide-copper(II) species, the formation of such species being previously suggested,[38,45] and the evidence for their formation was also obtained here. The recovered $V^{IV}O$ catalysts exhibit similar IR, electronic and EPR spectral patterns and these suggest that their original state is maintained after recovery. These polymeric supported catalysts are recyclable and do not leach into solution in any of the above catalytic reactions showing their heterogeneous nature. The EPR spectra obtained for the recovered Cu(II) catalysts indicate that the original state is not preserved after their use in the catalytic procedures.

Acknowledgements

The Council of Scientific and Industrial Research, New Delhi is gratefully acknowledged for financial support of the work. The authors also wish to thank FEDER, Fundação para a Ciência e a Tecnologia, POCI 2010 (namely PPCDT/QUI/55985/2004 and PPCDT/QUI/56946/2004 programs).

References

1 (*a*) T. Hirao, *Coord. Chem. Rev.*, 2003, **237**, 1; (*b*) T. Hirao, *Pure Appl. Chem.*, 2005, 1539–1557; (*c*) A. E. Shilov and G. B. Shul'pin, *Chem. Rev.*, 1997, **97**, 2879–2932; (*d*) A. G. J. Ligtenbarg, R. Hage and B. L. Feringa, *Coord. Chem. Rev.*, 2003, **237**, 89–101.
2 A. Butler, M. J. Clague and G. Meister, *Chem. Rev.*, 1994, **94**, 625–638.
3 K. Jahnisch, V. Hessel, H. Lowe and M. Baerns, *Angew. Chem., Int. Ed.*, 2004, **43**, 406–446.
4 H. Mimoun, L. Saussine, E. Daire, M. Postel, J. Fisher and R. Weiss, *J. Am. Chem. Soc.*, 1983, **105**, 3101–3110.
5 L. Canali and D. C. Sherrington, *Chem. Soc. Rev.*, 1999, **28**, 85–93.
6 Y. R. de Miguel, *J. Chem. Soc., Perkin Trans. 1*, 2000, 4213–4221.
7 N. E. Leadbeater and M. Marco, *Chem. Rev.*, 2002, **102**, 3217–3273.
8 T. Punniyamurthy and L. Rout, *Coord. Chem. Rev.*, 2008, **252**, 134–154.
9 B. Meunier, *Chem. Rev.*, 1992, **92**, 1411–1456.
10 D. C. Sherrington, in *Supported Reagents and Catalyst in Chemistry*, ed. B. K. Hodnett, A. P. Keybett, J. H. Clark, and K. Smith, Royal Society of Chemistry, Cambridge, 1998, p. 220.
11 M. A. Petit and J. Jozefonvicz, *J. Appl. Polym. Sci.*, 1977, **21**, 2589–2596.
12 V. B. Valodkar, G. L. Tembe, M. Ravindranathan, R. N. Ram and H. S. Rama, *J. Mol. Catal. A: Chem.*, 2004, **208**, 21–32.
13 M. R. Maurya and S. Sikarwar, *Catal. Commun.*, 2007, **8**, 2017–2024.
14 B. Fredrich, in *Ullmann's Encyclopedia of Industrial Chemistry*, ed. W. Gerhartz, Weinheim, New York, 1985, vol. A3, p. 470.
15 J. Schneider, DE-OS 2 026 817, 1970, assigned to Bayer.
16 H. Yamachika and H. Nakanishi, *Kaku Yugo Kenkyu*, 1982, **47**, 580–591.
17 C. Walling, C. Zhao and G. M. El-Taliawi, *J. Org. Chem.*, 1983, **48**, 4910–4914.
18 H. V. Borgaonkar and S. B. Chanadlia, *J. Chem. Technol. Biotechnol.*, 1984, **34A**, 107–112.
19 M. Constantini and L. Krumenacker, *Stud. Surf. Sci. Catal.*, 1989, **44**, 159–166.
20 I. Nishiguchi and T. Hirashima, *J. Org. Chem.*, 1985, **50**, 539–541.
21 A. P. Singh and T. Selvan, *J. Appl. Catal A.*, 1996, **143**, 111–124.
22 J. Wang, H. Fang, Y. Li, J. Li and Z. Yan, *J. Mol. Catal. A: Chem.*, 2006, **250**, 75–79.
23 (*a*) C. T. Dalton, K. M. Ryan, V. M. Wall, C. Bousquest and D. G. Gilheary, *Top. Catal.*, 1998, 575–591; (*b*) D. C. Sherrington, *Catal. Today*, 2000, **57**, 87–104, and references therein.
24 (*a*) B. B. De, B. B. Lohray, S. Sivaram and P. K. Dhal, *Macromolecules*, 1994, **27**, 1291–1296; (*b*) B. B. De, B. B. Lohray, S. Sivaram and P. K. Dhal, *Tetrahedron: Asymmetry*, 1995, **6**, 2105–2108.
25 (*a*) M. D. Angelino and P. E. Laibinis, *J. Polym. Sci., Part A: Polym. Chem.*, 1999, **37**, 3888–3898; (*b*) C. E. Song, E. J. Roh, B. M. Yu, D. Y. Chi, S. C. Kim and K.-J. Lee, *Chem. Commun.*, 2000, **25**, 615–616; (*c*) J. Tong, Y. Zhang, Z. Li and C. Xia, *J. Mol. Catal. A: Chem.*, 2006, **249**, 47–52.
26 (*a*) M. R. Maurya, U. Kumar and P. Manikandan, *Dalton Trans.*, 2006, 3561–2575; (*b*) M. R. Maurya, U. Kumar and P. Manikandan, *Eur. J. Inorg. Chem.*, 2007, 2303–2314.
27 C. E. Housecroft, and A. G. Sharpe, *Inorganic Chemistry*, Prentice Hall, London, 2001, p. 466–470.
28 J. C. Duff and E. J. Bills, *J. Chem. Soc., Trans.*, 1923, **5**, 1987.
29 A. Rockenbauer and L. Korecz, *Appl. Magn. Reson.*, 1996, **10**, 29–43.
30 C. Gruning and D. Rehder, *J. Inorg. Biochem.*, 2000, **80**, 185–189.
31 S. Abe, T. Ueno, P. A. N. Reddy, S. Okazaki, T. Hikage, A. Suzuki, T. Yamane, H. Nakajima and Y. Watanabe, *Inorg. Chem.*, 2007, **46**, 5137–5139.
32 I. Cavaco, J. Costa Pessoa, M. T. Duarte, R. T. Henriques, P. M. Matias and R. D. Gillard, *J. Chem. Soc., Dalton Trans.*, 1996, 1989–1996.
33 J. Costa Pessoa, M. J. Calhorda, I. Cavaco, I. Correia, M. T. Duarte, V. Felix, R. T. Henriques, M. F. M. Piedade and I. Tomaz, *J. Chem. Soc., Dalton Trans.*, 2002, 4407–4415.
34 P. Arroyo, S. Gil, A. Munoz, P. Palanca, J. Sanchis and V. Sanz, *J. Mol. Catal. A: Chem.*, 2000, **160**, 403–408.
35 D. Dolphin, and A. Wick, *Tabulation of Infrared Spectral Data*, Wiley-Interscience, New York, 1977, pp. 288, 303, 304.
36 R. H. Holm, P. Kennepohl and E. I. Solomon, *Chem. Rev.*, 1996, **96**, 2239–2314.
37 J. D. Koola and J. K. Kochi, *J. Org. Chem.*, 1987, **52**, 4545–45553.
38 W. Nam, R. Ho and J. S. Valentine, *J. Am. Chem. Soc.*, 1991, **113**, 7052–7054.
39 K. Nakajima, M. Kojima, K. Toriumi, K. Saito and J. Fujita, *Bull. Chem. Soc. Jpn.*, 1989, **62**, 760–767.
40 K. Nakajima, K. Kojima, M. Kojima and J. Fujita, *Bull. Chem. Soc. Jpn.*, 1990, **63**, 2620–2630.

41 M. R. Maurya, *Coord. Chem. Rev.*, 2003, **237**, 163–181.

42 S. Dutta, S. Mondal and A. Chakravorty, *Polyhedron*, 1995, **14**, 1163–1168.

43 M. Bonchio, V. Conte, F. di Furia, G. Modena, S. Moro and J. O. Edwards, *Inorg. Chem.*, 1994, **33**, 1631–1637.

44 C. Djordjevic, M. Lee and E. Sinn, *Inorg. Chem.*, 1989, **28**, 719–723.

45 V. Vergopoulos, W. Priebsch, M. Fritzsche and D. Rehder, *Inorg. Chem.*, 1993, **32**, 1844–1849.

46 R. Fulwood, H. Schmidt and D. Rehder, *J. Chem. Soc., Chem. Commun.*, 1995, 1443–1444.

47 M. R. Maurya, U. Kumar, I. Correia, P. Adão and J. Costa Pessoa, *Eur. J. Inorg. Chem.*, 2008, 577–587.

48 (*a*) E. I. Solomon, P. Chen, M. Metz, S.-K. Lee and A. E. Palner, *Angew. Chem., Int. Ed.*, 2001, **40**, 4570–4590; (*b*) J. P. Klinman, *Chem. Rev.*, 1996, **96**, 2541–2561.

49 K. D. Karlin, J. C. Hayes, Y. Gultneh, R. W. Cruse, J. W. McKown, J. P. Hutchinson and J. Zubieta, *J. Am. Chem. Soc.*, 1984, **106**, 2121–2128.

50 H. Mimoun, M. Mignard, P. Brechot and L. Saussine, *J. Am. Chem. Soc.*, 1986, **108**, 3711–3718.

51 M. Bonchio, V. Conte, F. di Furia and G. Modena, *J. Org. Chem.*, 1989, **54**, 4368–4371.

52 (*a*) G. B. Shul'pin, D. Attanasio and L. Suber, *J. Catal.*, 1993, **142**, 147–152; (*b*) D. Attanasio, L. Suber and G. B. Shul'pin, *Bull. Russ. Acad. Sci. Div. Chem. Sci.*, 1992, **41**, 1502–1504.